



# SBGf Conference

18-20 NOV | Rio'25

**Sustainable Geophysics at the Service of Society**

**In a world of energy diversification and social justice**

**Submission code: 405D6NGRVA**

See this and other abstracts on our website: <https://home.sbgf.org.br/Pages/resumos.php>

## **Seismic anisotropy assessment using angle-domain common image gathers**

**Ammir Karsou (GISIS/UFF), Felipe Costa (GISIS/UFF), Felipe Capuzzo (GISIS / UFF), Rodrigo Stern (GISIS/UFF), Marco Cetale (GISIS/UFF), Roger Moreira (GISIS / UFF)**

## Seismic anisotropy assessment using angle-domain common image gathers

Copyright 2025, SBGf - Sociedade Brasileira de Geofísica / Society of Exploration Geophysicist.

This paper was prepared for presentation during the 19<sup>th</sup> International Congress of the Brazilian Geophysical Society held in Rio de Janeiro, Brazil, 18-20 November 2025. Contents of this paper were reviewed by the Technical Committee of the 19<sup>th</sup> International Congress of the Brazilian Geophysical Society and do not necessarily represent any position of the SBGf, its officers or members. Electronic reproduction or storage of any part of this paper for commercial purposes without the written consent of the Brazilian Geophysical Society is prohibited.

### Abstract

Angle-domain common image gather (ADCIG) is an effective up-to-date tool for imaging workflows. It serves as a velocity model quality control, being sensitive to velocity inaccuracies, an inaccurate modeling equation, and can be used to enhance the final image by selectively stacking traces with similar amplitudes. The calculation can be done during reverse time migration (RTM), decomposing source and receiver wavefields into propagation angle sectors, the correlation of these angle sectors generate the resulting angle gathers. The results show that isotropic migration generates a shifting pattern in angle gathers when the data have VTI anisotropy, which is correctly flattened when the VTI wave equation kernel is incorporated in the migration process. This work implements ADCIGs in 2D and shows that they can be used to quantitatively estimate the impact of the anisotropy on the final image and can be used to correct angle gathers when with correct anisotropic parameters.

### Introduction

RTM has been widely used due to its capabilities, which allows the use of complex wave propagation effects such as dipping structures, complex geology, and anisotropic effects. In most scenarios, traditional isotropic wave equation is able to generate clean results, but in the presence of anisotropy it can lead to incorrect events and artifact generation in the final stack. ADCIG is a tool that is capable of acting as a migration quality control, this is done by verifying the behavior of the seismic migration with respect to the angle of reflection and angle of azimuth (Biondi and Symes, 2004). In the presence of errors in the velocity model or wave equation, ADCIGs helps to assess how far it is from the solution by verifying how far the angle gathers are from being flat. In this work, we will generate ADCIGs using wavefield decomposition in the wavenumber domain with isotropic and vertical transverse isotropy (VTI) data to show the shift of angle gathers when using an inappropriate wave solution.

### Theory

#### VTI formulation

Wave propagation in anisotropic media can be described using the elastic velocity-stress formulation, expressed as:

$$\begin{cases} \partial_t v_i - \frac{1}{\rho} \partial_j \sigma_{ij} = \frac{1}{\rho} f_i, \\ \partial_t \sigma_{ij} = C_{ijkl} \frac{1}{2} (\partial_k v_l + \partial_l v_k) - \partial_t g_{ij}. \end{cases} \quad (1)$$

The coefficients  $C_{ijkl}$  are defined by a fourth order stiffness tensor. In general anisotropy, the matrix is full and equations will use all coefficients in its formulation. When using VTI symmetry, we can eliminate some terms and simplify the resulting matrix in 2D using Voigt notation as:

$$C_{IJ} = \begin{bmatrix} C_{11} & C_{13} & 0 \\ C_{13} & C_{33} & 0 \\ 0 & 0 & C_{55} \end{bmatrix}.$$

The indices  $I$  and  $J$  in the Voigt notation correspond to specific pairs of tensor indices  $(ij, kl)$  following the mapping conventions for symmetric elasticity matrices. We can define the stiffness components as functions of P-wave velocity, S-wave velocity and the Thomsen anisotropic parameters. Using this approach, we can obtain the coefficients in the form:

$$C_{11} = (\lambda + 2\mu)(2\epsilon + 1), \quad (2a)$$

$$C_{33} = (\lambda + 2\mu), \quad (2b)$$

$$C_{55} = \mu, \quad (2c)$$

$$C_{13} = \sqrt{2\delta C_{33}(C_{33} - C_{55}) + (C_{33} - C_{55})^2} - C_{55}, \quad (2d)$$

where  $\lambda$  and  $\mu$  are the first and second Lamé parameters,  $\epsilon$  and  $\delta$  are the Thomsen anisotropic parameters. This formulation provides a fundamental framework for describing the elastic properties of VTI media. In this work, we simulate acoustic seismic data setting with  $\mu = 0$ , which will result in an acoustic data.

### ADCIG calculation

ADCIGs can be calculated using either poynting vectors or by local plane-wave decomposition (LPWD). The LPWD method divides the wavefront into portions of different propagation angles, generally using Fourier Transform (FT). The relation of the wavenumbers  $k_x$  and  $k_z$  gives us the propagation angle of the wavefront, which we can use to separate different propagation angles. Following Jin et al. (2020) approach, we calculate a predefined set of angle sectors, apply them to the wavenumber domain and get its respective propagation angle by using an inverse FT. This step is done during the imaging process and the workflow can be described as:

1. Transform the space-time domain source and receiver wavefields  $P_s(x, t)$  and  $P_r(x, t)$  into the wavenumber time domain  $P_s(\mathbf{k}, t)$  and  $P_r(\mathbf{k}, t)$  by 2D Fourier transform.
2. Divide the source and receiver wavenumbers into a certain number of sectors based on a pre-defined propagation directions  $\beta_1$  and  $\beta_2$ ,  $P_s(\mathbf{k}, t, \beta_1)$  and  $P_r(\mathbf{k}, t, \beta_2)$ .
3. Apply an inverse Fourier transform to the sectored wavenumbers back into the space-time domain with the assigned propagation angle  $P_s(\mathbf{k}, t, \beta_1)$  and  $P_r(\mathbf{k}, t, \beta_2)$ .
4. Cross-correlate the decomposed source and receiver wavefields and bin each image into calculated reflection angle given by the relation:  $\theta = \frac{|\beta_1 - \beta_2|}{2}$ .

The sectors are calculated from  $0^\circ$  to  $60^\circ$  in every  $10^\circ$ , a  $2^\circ$  window taper is used for each sector with a profile function used in Mallat (2009) to construct lapped orthogonal transforms. The imaging condition used is the Claerbout (1971) deconvolution imaging condition and the results were filtered in the wavenumber domain using a low-cut filter to remove the backscattering artifacts.

### Results

The data used in this work were simulated using the VTI elastic wave equation, using elastic rock property models based on the Hess VTI migration benchmark (Figure 1). The benchmark includes P-velocity, density, epsilon and delta, and S-velocity models, S-velocity with is set to zero. The acquisition geometry consists of sources at every 100 m and receivers at every 10 m, modeled with no free-surface multiples with 7 s of record with a 1 millisecond time step. The wavelet used was a ricker with cut frequency of 30 Hz and dominant frequency of 10 Hz.

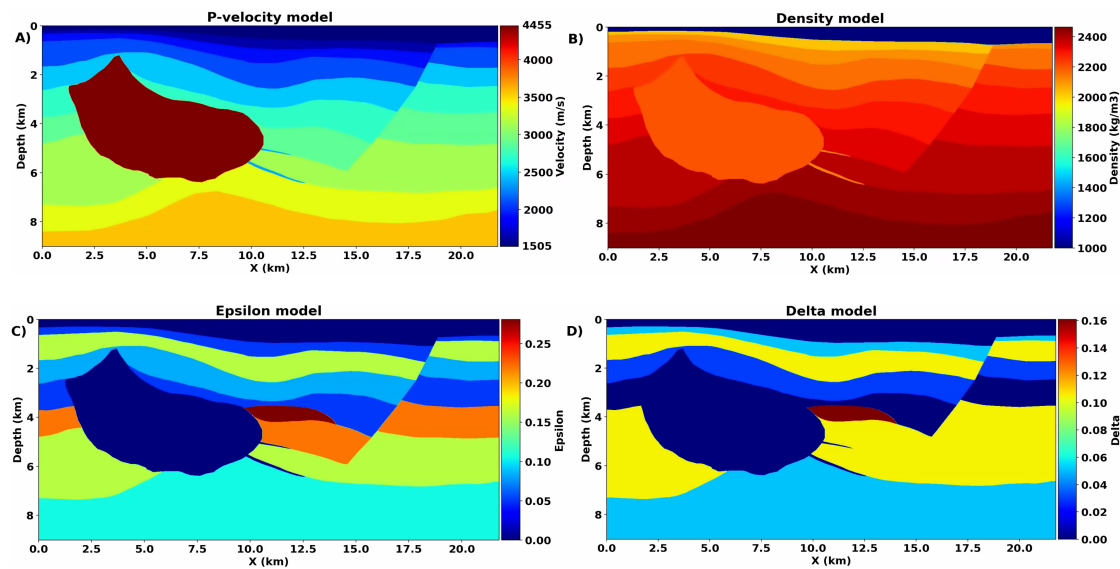


Figure 1: Hess VTI property models used for data modeling and migration: a) P-velocity. b) Density. c) Epsilon. d) Delta.

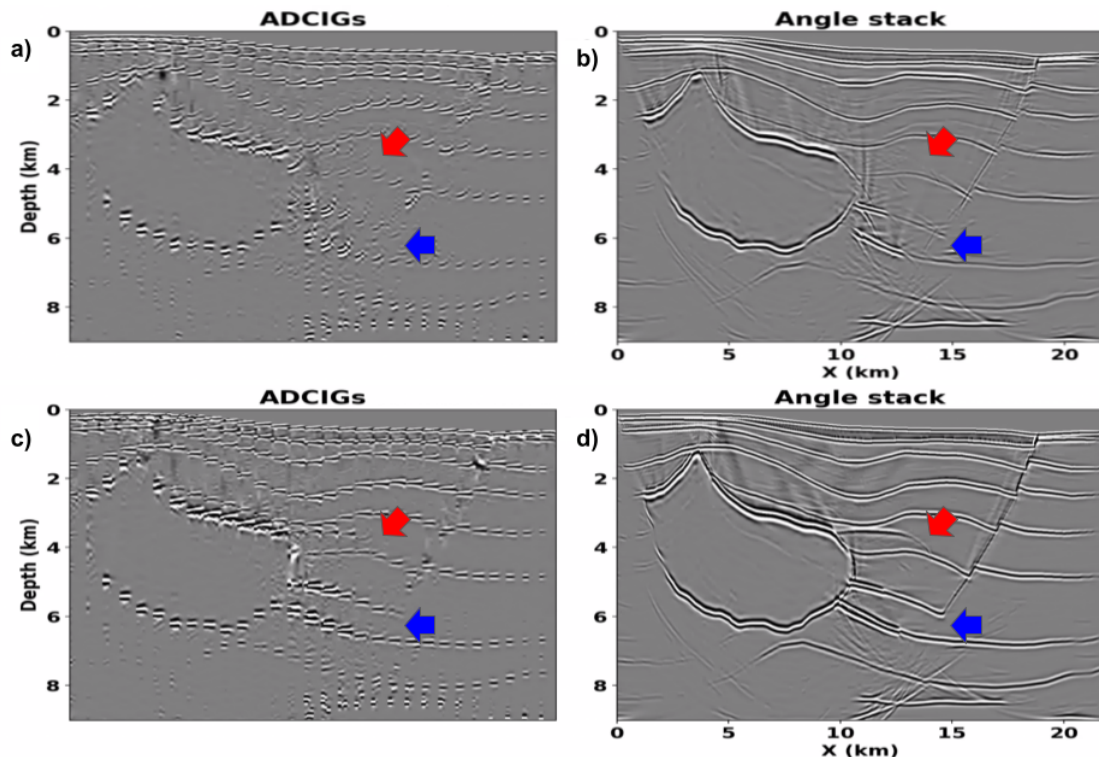


Figure 2: Comparison of ADCIGs and its stack using isotropic and VTI equations: a) ADCIGs for isotropic RTM. b) Angle stack of isotropic RTM. c) ADCIGs for VTI RTM. d) Angle stack of VTI RTM.

The results showing the ADCIGs and the stacked image using isotropic wave equation is shown in figure 2(a). We can see that in the shallow region, where there is no presence of anisotropy, ADCIGs are flat. But for deeper regions we can see the effect of anisotropy appearing as an upward shift on ADCIGs, which means that migration velocity used in migration is slower than should be, due to anisotropic changes of velocity. On the stacked image we can see that there is a lack of amplitude

continuity on reflectors, specially in the reservoir region (blue arrow) due to it being located below an anisotropic layer (red arrow). When we generate the ADCIGs using correct wave equation (figure 2(c)), we can see that the overall angle gather positioning is corrected, also we can see that the anisotropic layer (red arrow) is delimitated, which does not occur on figure 2(a). In the stacked image, we see that the reflectors now show good amplitude continuity, due to the flattening of the gathers, showing appropriate account of anisotropic effects into the migration algorithm. This is shown in the reservoir region, where its position was correct right below the salt and also improving the amplitude continuity of the nearby layers. The image gain also improves the image on the fault area, showing better delimitation of the fault due to correct amplitude positioning alongside it.

### Conclusions

The results showed that ADCIGs are able to detect anisotropic effects in reverse time migration, generating correcting its positioning when accounting correct wave equation. This shows that RTM ADCIG analysis is a powerful tool in migration QC, highlighting the errors when incorrect velocity or wave equation are used. Future work will take into account the effect of shear wave effects, showing the impact of wave conversion on angle gathers.

### Acknowledgments

The authors from Fluminense Federal University acknowledge the financial support from Petrobras through the R&D project “Modelagem Visco-Elástica Anisotrópica em Dados Multi-Azimutais para Análise de Sensibilidade de Sistemas de Fraturas” (ANP no. 24643-9). The strategic importance of the R&D levy regulation of the National Agency for Petroleum, Natural Gas and Biofuels (ANP) is gratefully appreciated.

### References

- Biondi, B., and W. W. Symes, 2004, Angle-domain common-image gathers for migration velocity analysis by wavefield-continuation imaging: *GEOPHYSICS*, **69**, 1283–1298.
- Claerbout, J. F., 1971, Toward a unified theory of reflector mapping: *Geophysics*, **36**, 467–481.
- Jin, H., P. Vu, Q. Liao, Z. Yu, and C. Chu, 2020, *in* 3D RTM sparse angle gathers: 3053–3057.
- Mallat, S., 2009, *A wavelet tour of signal processing: The sparse way*: Elsevier Press.